Cell, Vol. 75, 855–862, December 3, 1993, Copyright © 1993 by Cell Press

Posttranscriptional Regulation of the Heterochronic Gene *lin-14* by *lin-4* Mediates Temporal Pattern Formation in C. elegans

Bruce Wightman,*† Ilho Ha,* and Gary Ruvkun
Department of Molecular Biology
Massachusetts General Hospital
Boston, Massachusetts 02114

Summary

During C. elegans development, the temporal pattern of many cell lineages is specified by graded activity of the heterochronic gene *Lin-14*. Here we demonstrate that a temporal gradient in Lin-14 protein is generated posttranscriptionally by multiple elements in the *lin-14* 3′UTR that are regulated by the heterochronic gene *Lin-4*. The *lin-14* 3′UTR is both necessary and sufficient to confer *lin-4*-mediated posttranscriptional temporal regulation. The function of the *lin-14* 3′UTR is conserved between C. elegans and C. briggsae. Among the conserved sequences are seven elements that are each complementary to the *lin-4* RNAs. A reporter gene bearing three of these elements shows partial temporal gradient activity. These data suggest a molecular mechanism for Lin-14p temporal gradient formation: the *lin-4* RNAs base pair to sites in the *lin-14* 3′UTR to form multiple RNA duplexes that down-regulate *lin-14* translation.

Introduction

The heterochronic genes of Caenorhabditis elegans form a regulatory hierarchy that coordinately controls the temporal identities of cells during development (Ambros, 1989). Like the Drosophila anterior–posterior and dorsal–ventral axis determination genes that control cell identities specifically in their respective axes (Nüsslein-Volhard, 1991), heterochronic genes point to a third orthogonal axis under explicit genetic control, that of time. The heterochronic gene pathway generates a temporal gradient of Lin-14 protein (Lin-14p) that specifies the normal temporal sequence of cell lineages (Ruvkun and Giusto, 1989). Mutations in the heterochronic genes *lin-4*, *lin-14*, *lin-28*, and *lin-29* cause temporal transformations of cell lineage in many tissues and cell types (Chalfie et al., 1981; Ambros and Horvitz, 1984). Depending on the mutation, stage-specific cell lineages in heterochronic mutant animals occur at either earlier or later stages than they would normally. These mutations perturb temporal patterning by disrupting the regulation of, or response to, the Lin-14p temporal gradient. A key question in temporal pattern formation is how the heterochronic gene pathway generates this molecular gradient.

The instructive role of *lin-14* in temporal pattern formation was established by the observation that *lin-14* gain-of-function (gf) and loss-of-function (lf) mutations have opposite phenotypes (Ambros and Horvitz, 1987). *lin-14(lf)* alleles cause larvae stage 2 (L2) patterns of cell lineage in a variety of tissues to be executed precociously during the L1 stage (Ambros and Horvitz, 1987). Two *lin-14(gf)* alleles cause the opposite transformation in temporal cell fate, reiterations of early cell fates at later stages. For instance, at the L2 stage, *lin-14(gf)* mutants repeat patterns of cell lineage appropriate for the L1 stage (Ambros and Horvitz, 1984).

lin-14 controls these stage-specific cell lineages by generating a temporal gradient of Lin-14 nuclear protein (Lin-14p). Lin-14p levels are high during the L1 stage but are faintly detectable by indirect immunofluorescence at L2 and later stages (Ruvkun and Giusto, 1989). The *lin-14(gf)* mutations interfere with *lin-14* temporal down-regulation, causing inappropriately high Lin-14p levels at post-L1 stages, which imposes L1 patterns of cell lineage on post-L1 blast cells (Ruvkun and Giusto, 1989). These mutations delete sequences from the *lin-14* mRNA 3′ untranslated region (3′UTR), suggesting that regulatory elements in the 3′UTR normally are responsible for mediating the down-regulation of Lin-14p abundance at later larval stages (Wightman et al., 1991).

The heterochronic gene *lin-4* is a negative regulator of *lin-14* (Ambros, 1989; Arasu et al., 1991). A null mutation in *lin-4* results in L1-specific cell lineage reiterations similar to those observed with *lin-14(gf)* mutations and causes Lin-14p to be present at post-L1 stages (Chalfie et al., 1981; Arasu et al., 1991; Lee et al., 1993 [this issue of *Cell*]). In addition, *lin-14* gene activity is necessary for the Lin-4 heterochronic defects (Ambros, 1989). Therefore, the *lin-4* gene product is required for normal temporal regulation of Lin-14p and is a candidate for directly interacting with negative regulatory elements in the *lin-14* 3′UTR identified by *lin-14(gf)* mutations. The functional products of the *lin-4* gene are two small untranslated RNA molecules (Lee et al., 1993).

Here we examine the molecular mechanism by which the Lin-14p temporal gradient is generated. We find that temporal regulation of Lin-14p abundance during wild-type development occurs at a posttranscriptional step and is mediated by the *lin-14* 3′UTR that bears multiple conserved elements complementary to the *lin-4* RNAs. These data suggest that the Lin-14p temporal gradient is generated by *lin-4* antisense base pairing to the *lin-14* mRNA.

Results

Down-Regulation of Lin-14p Occurs at a Posttranscriptional Step

To obtain a quantitative description of the temporal regulation of Lin-14p previously observed in indirect immunofluorescence experiments (Ruvkun and Giusto, 1989; Arasu et al., 1991), immunoblots were performed using protein extracts from synchronized wild-type, *lin-14(gf)*, and *lin-4* mutant animals. Early stage preparations (71%–89%, L1 stage) and late stage preparations (78%–94%, L2 and L3 stages) were prepared from wild-type and mutant strains.

*The first two authors contributed equally to this work.
†Present address: Department of Molecular and Cell Biology, University of California at Berkeley, Berkeley, California 94720.

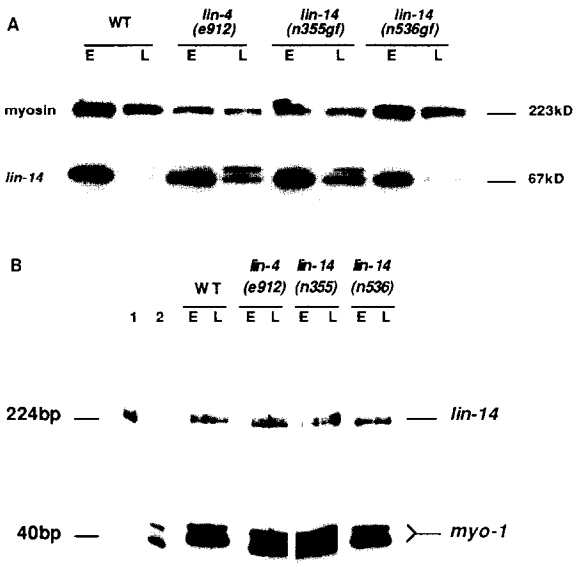

Figure 1. Posttranscriptional Generation of the Lin-14p Temporal Gradient

(A) Immunoblot analysis of Lin-14p levels in synchronized preparations from wild-type and heterochronic mutants. Protein extracts were prepared from wild-type and *lin-4(e912)*, *lin-14(n355gf)*, and *lin-14(n536gf)* mutants. Early stage (E) preparations were 71%–89% L1 stage. Late stage (L) preparations were 78%–94% L2 and L3 stages. Blots were probed with a monoclonal antibody to the pharyngeal myosin isoform myo-1 and with a polyclonal anti-Lin-14p antiserum. The anti-Lin-14p antibodies detect bands at 67 kd and 70 kd that are specific to Lin-14p. For quantitation purposes, the intensities of both species were determined in 5 independent blots by densitometry, summed, and normalized to the intensity of the 223 kd pharyngeal myosin product. The ratio of Lin-14p levels at late stages to early stages for each genotype is as follows: wild-type, 0.1; *lin-4(e912)*, 0.4; *lin-14(n355)*, 0.7; *lin-14(n536)*, 0.4.

(B) RNAase protection of RNA from staged wild-type and heterochronic mutant animals. Total RNA was made from the same synchronized samples used in the immunoblot experiments and hybridized to antisense *lin-14* and *myo-1* probes. The *lin-14* probe was generated from a cDNA that spans exons 12 and 13 (bases 19476–19750) and detects a 224 nt fragment. The *myo-1* probe detects a 40 nt RNA fragment. A doublet was observed with both probes, and the intensities of both bands were summed. The ratio of late to early stage *lin-14* RNA levels in the same preparations analyzed in (A) are as follows: wild-type, 1.0; *lin-4(e912)*, 0.91; *lin-14(n355)*, 1.5; and *lin-14(n536)*, 1.2. The 1.2-fold and 1.5-fold increase in *lin-14* RNA levels in the *lin-14(n536gf)* and *lin-14(n355gf)* mutants, respectively, are too small to interpret as significant. The figure shown is a composite.

Relative to pharyngeal myosin control, Lin-14p levels decrease by a factor of 10 between early and late stages in wild-type (Figure 1A). In contrast, relative Lin-14p levels decrease by a factor of 2.3 in *lin-14(n536gf)* and *lin-4(e912)* mutants and decrease by a factor of 1.3 in the *lin-14 (n355gf)* mutant. Therefore, both *lin-14(gf)* and *lin-4* mutants cause a 4- to 7-fold increase in the abundance of Lin-14p at later stages as compared with wild type.

To establish whether *lin-14* is regulated at a transcriptional or posttranscriptional level, RNA was prepared from the same staged samples used for protein analysis, and the level of *lin-14* RNA relative to pharyngeal myosin RNA in each synchronized preparation was analyzed by RNAase protection (Figure 1B). In wild type, *lin-14* transcript abundance relative to pharyngeal myosin mRNA does not change significantly between early and late stages. Therefore, changes in steady-state RNA levels do not account for the 10-fold reduction in protein levels observed in wild type. In the two *lin-14(gf)* mutants and in the *lin-4* mutant, the *lin-14* transcript levels at both early and late stages are similar to wild type and, like wild type, show no dramatic temporal regulation.

These data show that *lin-14* is temporally regulated at a posttranscriptional step other than transcript stability in wild-type animals; the *lin-14(gf)* mutations act by disrupting this posttranscriptional regulation; and the *lin-4* product also acts at a posttranscriptional step.

The *lin-14* 3′UTR Is Sufficient for Temporal Regulation

To test whether the *lin-14* 3′UTR alone is capable of conferring temporal regulation on another gene, we compared its activity on a *lacZ* reporter gene in C. elegans with that of a control 3′UTR. The reporter gene uses the promoter of the *col-10* collagen gene that is active in hypodermal cells that accumulate Lin-14p (Ruvkun and Giusto, 1989) and that are affected by *lin-14* mutations (Ambros and Horvitz, 1984). We utilized the 3′UTR from the *unc-54* myosin gene (Dibb et al., 1985) as a control. Strains bearing these transgenes were assayed at each larval stage for β-galactosidase activity in extracts and by X-Gal staining of whole-mount fixed animals.

Reporter genes bearing the *lin-14* 3′UTR showed 100- to 180-fold down-regulation between the L1 and L4 stages (Table 1). The dramatic down-regulation between the L1 and L4 stages also is observable in X-Gal-stained fixed animals bearing these transgenes (Figure 2). There was no detectable down-regulation of β-galactosidase activity or X-Gal staining from the *lin-14* 3′UTR transgenes between the L1 and L2 stages, perhaps owing to perdurance of the β-galactosidase protein (data not shown). Between the L1 and the L4 stage, β-galactosidase activity produced from the control *unc-54* 3′UTR reporter gene decreased by a factor of 7 (Table 1). X-Gal staining of whole-mount animals bearing this transgene shows that all stages from late embryo to adult express *lacZ* in hypodermal cells (Figure 2). Thus, the reporter genes bearing a *lin-14* 3′UTR showed 14- to 25-fold greater temporal down-regulation than the control *unc-54* 3′UTR reporter construct.

RNAase protection analysis shows no temporal decrease in *col-10–lacZ–lin-14* mRNA levels between the L1 and L4 stages in strains bearing the reporter gene (Figure 3). These data suggest that the observed temporal down-regulation of *lacZ* expression occurs by the same posttranscriptional mechanism that operates on the *lin-14* mRNA in wild type. In addition, these data suggest that the *col-10* promoter activity is not temporally regulated, and that the 7-fold decrease in *lacZ* activity observed with the *unc-54* 3′UTR transgene probably reflects a low level of posttranscriptional regulation conferred by this control 3′UTR.

β-Galactosidase activity also was down-regulated by a factor of about 100 between the L1 to the L4 stages in a wild-type

Table 1. β-Galactosidase Activity of the Fusion Constructs in Staged Preparations from Transgenic Animals.

β′UTR	Genotype	β-Galactosidase Activity		
		L1	L4	L1/L4 ratio
lin-14	WT(int)	1.6 ± 0.9	0.02 ± 0.02	99 ± 33 (n = 4)
	lin-4(int)	1.0 ± 0.9	0.4 ± 0.4	4 ± 3 (n = 9)
	WT(Ex)	4.1 ± 2.0	0.02 ± 0.005	182 ± 60 (n = 3)
	WT(Ex)high	164 ± 49	1.6 ± 0.4	104 ± 15 (n = 3)
unc-54	WT(int)	9.0 ± 4.4	1.4 ± 0.7	7 ± 4 (n = 4)
	lin-4(int)	0.4 ± 0.3	0.2 ± 0.02	2 ± 1 (n = 2)
lin-14/802 nt	WT(Ex)high	108 ± 25	1.6 ± 0.8	72 ± 16 (n = 3)
lin-14/124 nt	WT(Ex)high	116 ± 7	1.7 ± 0.3	72 ± 16 (n = 2)

Each construct utilizes a *col-10* promoter fused to *lacZ* with different 3′UTRs. The activity of these constructs was determined in either wild-type or *lin-4* mutant backgrounds, as indicated. The transgene arrays were analyzed as either extrachromosomal array (Ex) or randomly integrated into a chromosome (int). Those transgenes assayed as high copy arrays are indicated by high and have higher β-galactosidase activity. The units shown are change of OD_{574} from CPRG hydrolysis per minute per milligram of protein and are mean values and standard deviations. The ratio of L1 to L4 β-galactosidase activity was calculated for each experiment, and the mean and standard deviations are shown.

strain bearing a high copy *col-10–lacZ–lin-14* transgene extrachromosomal array (Table 1). This pC10L14 plasmid was injected into wild type at 50-fold higher DNA concentration than the transgenes described above, and β-galactosidase activity at both the L1 and L4 stages was 60–80 times that of the corresponding stages for strains bearing a low-copy transgene array, suggesting that the high copy transgene array in fact expresses much more *col-10–lacZ–lin-14* mRNA. These data suggest that the trans-acting factors that mediate this down-regulation cannot be saturated by a more than 50-fold increase in *lin-14* mRNA level. Consistent with this observation, we observed no increase in Lin-14p levels at post-L1 stages and no Lin-14(gf) phenotypes in wild-type strains bearing the high copy transgene (data not shown).

Negative regulatory activity in the *lin-14* 3′UTR was mapped more precisely with the pC10L14/802 and pC10-L14/124 constructs that contain, respectively, 802 nt (position 20244 to 21046 in Wightman et al., 1991) and 124 nt (position 20696 to 20810) *lin-14* 3′UTR regions placed in an *unc-54* 3′UTR context. These *lin-14* 3′UTR regions were selected for analysis based on conserved sequence elements (see below). Strains bearing either of these constructs showed a level of temporal down-regulation (72-fold) intermediate between the *unc-54* 3′UTR and the full *lin-14* 3′UTR. These data show that some but not all of the *lin-14* temporal gradient generating activity maps to the 124 nt region of the *lin-14* 3′UTR and that this activity can act in the context of an *unc-54* 3′UTR, including its polyadenylation site.

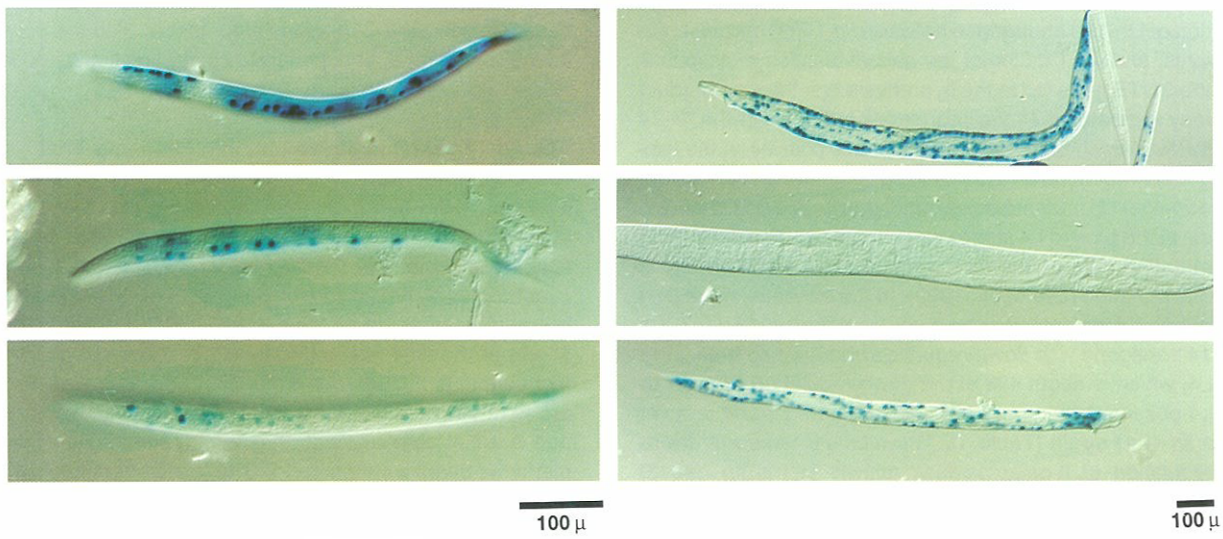

Figure 2. Temporal Regulation of *lacZ* Reporter Genes in Whole-Mount C. elegans Preparations

L1 animals are on the left and L4 animals on the right.

(Top) *col-10–lacZ–unc-54* in wild type, showing X-Gal staining at both the L1 and L4 stages.

(Middle) *col-10–lacZ–lin-14* in wild type, showing only L1 expression of the transgene. The L4 animal carried a transgene as determined by the twist in the cuticle and ventral cord caused by the *rol-6(gf)* gene.

(Bottom) *col-10–lacZ–lin-14* in *lin-4(e912)*, showing that the transgene expresses at both the L1 and L4 stages in a *lin-4(e912)* mutant.

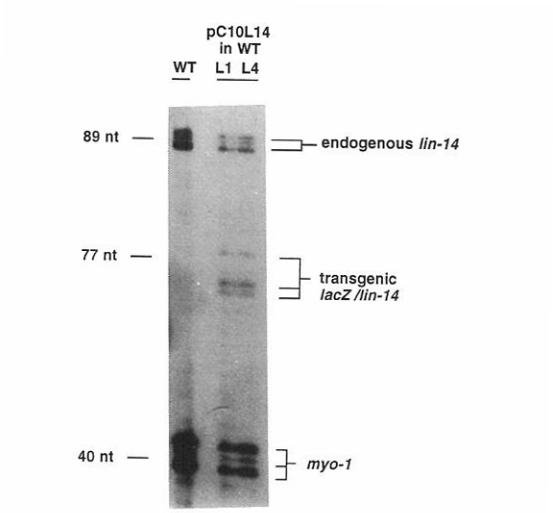

Figure 3. RNA Levels from Transgenic Animals Carrying the *col-10–lacZ–lin-14* 3′UTR Fusion Gene

The left lane is total RNA prepared from mixed-stage wild-type animals. The right two lanes are staged L1 and L4 RNAs from a strain that bears an integrated pC10L14 construct in an otherwise wild-type background. In each case, 10 μg of total RNA was hybridized to two labeled antisense RNA probes: one complementary to *myo-1*, as an internal control, that protects a 40 bp fragment as described in Figure 1B, and the other complementary to a portion of the 3′ end of the *lin-14* gene. The *lin-14* probe spans the region that is fused to *lacZ* in construct pC10L14, and protects an 89 bp portion of endogenous full-length *lin-14* RNA and a 77 bp portion of RNA produced from the transgenic *col-10–lacZ–lin-14* 3′UTR fusion mRNA. The ratio of L1 to L4 transgenic *col-10–lacZ–lin-14* mRNA levels relative to myosin was 0.9 in this experiment. Similar results were obtained using a probe complementary to *lacZ* (data not shown).

lin-4 Is Required for Down-Regulation Via the *lin-14* 3′UTR

The similarities in the cell lineage defects and in the regulation of Lin-14p abundance between *lin-14(gf)* and *lin-4* mutants, and the location of the gain-of-function mutations in the 3′UTR have led to the hypothesis that the *lin-4* product may regulate *lin-14* via sequences in 3′UTR of the *lin-14* mRNA (Arasu et al., 1991). To test this possibility, the integrated transgene arrays analyzed above were crossed into a *lin-4(e912)* mutant background, and β-galactosidase levels at the L1 and L4 stages were analyzed. The *lin-4(e912)* mutation deletes the *lin-4* transcripts and is therefore a null mutation (Lee et al., 1993). In the absence of the *lin-4* product, β-galactosidase activity from the *col-10–lacZ–lin-14* transgene was down-regulated about 4-fold from L1 to L4, which is about 4% of the down-regulation from L1 to L4 observed with the same integrated transgene array in a *lin-4(+)* strain (Table 1). The residual temporal down-regulation of β-galactosidase activity in the *lin-4(e912)* strain bearing the *lin-14* 3′UTR reporter gene was similar to that observed in the *unc-54* 3′UTR reporter gene in wild-type or *lin-4(e912)* strains. X-Gal staining of the *lin-4(e912)* strain bearing a *lin-14* 3′UTR transgene confirmed this result; hypodermal cells at all stages showed high level *lacZ* expression, unlike the same transgene in wild type (see Figure 2). Similar results were obtained with the *lin-4(ma161)* point mutant (Lee et al., 1993) (data not shown). Thus, the normally 100- to 200-fold temporal decrease in *lacZ* activity mediated by the *lin-14* 3′UTR is dependent upon *lin-4*.

The Function and Sequence of Elements in the *lin-14* 3′UTR Are Conserved between Species

For C. elegans, the related species C. briggsae has proven useful to detect conserved and possible functional residues in regulatory regions (Zucker-Aprison and Blumenthal, 1989). The Lin-14p temporal gradient is generated in C. briggsae, and the C. elegans *lin-14* 3′UTR can recapitulate a temporal gradient in C briggsae. Indirect immunofluorescence staining of C. briggsae animals using anti-LIN-14 antibody shows that L1 larvae accumulate Lin-14p, but by L2 and later stages, the protein is nearly undetectable (Figure 4). X-Gal staining of C. briggsae bearing a *lin-14* 3′UTR reporter gene showed little or no expression in L3, L4, and later animals, whereas L1 animals expressed high levels of β-galactosidase (Figure 4). With the *unc-54* 3′UTR, *lacZ* reporter gene expression could be detected at all stages in C. briggsae. Therefore, 3′UTR sequences or structures required for temporal down-regulation of *lin-14* are conserved between the two species.

Conserved elements in the *lin-14* 3′UTR were identified by sequencing the region from C. briggsae and comparing it with the C. elegans sequence (Figure 5). Multiple blocks of conserved sequence, separated by stretches with no conservation, are observed throughout the 3′UTR. The region that is deleted in both *lin-14(gf)* mutations (20173–21521; Wightman et al., 1991) contains conserved blocks of various lengths up to 30 nt. Additional conserved blocks of sequence are found between the *n536* 3′ deletion breakpoint and the polyadenylation signal (20824–21520). The regions of the *lin-14* mRNA that are not conserved highlight the extent of sequence divergence possible. Almost no sequence conservation was found in the 600 bases flanking the C. elegans stop codon, 3′ to the polyadenylation signal, at degenerate codon positions, and in introns.

The *lin-14* 3′UTR Includes Multiple Elements That Are Complementary to *lin-4*

Two small RNA products from the *lin-4* locus have been identified and characterized (Lee et al., 1993). Among the conserved regions in the *lin-14* 3′UTR are seven nearly exact copies of the 9 nt core element CUCAGGGAA, which is complementary to the sequence UUCCCUGAG at the 5′ end of the *lin-4* RNAs (Figure 5). In the *lin-14* mRNA, two elements include the entire 9 nt core element, four are 8 nt single base variants of the core element, and one is a 7 nt core element. In addition, all but one of the elements bears a conserved C 3′ to the *lin-4* complementary site that could base pair to a *lin-4*-encoded G if the RNA is 1 base longer than that suggested by RNA mapping experiments (see Lee et al., 1993). Upstream of these core sites on the *lin-14* mRNA are 5–9 nt sequences that are complementary to positions further 3′ on the *lin-4* RNAs (Figure 5).

All seven of the *lin-4*-complementary sites map to the 802 bp *lin-14* 3′UTR region in the pC10L14/802 construct

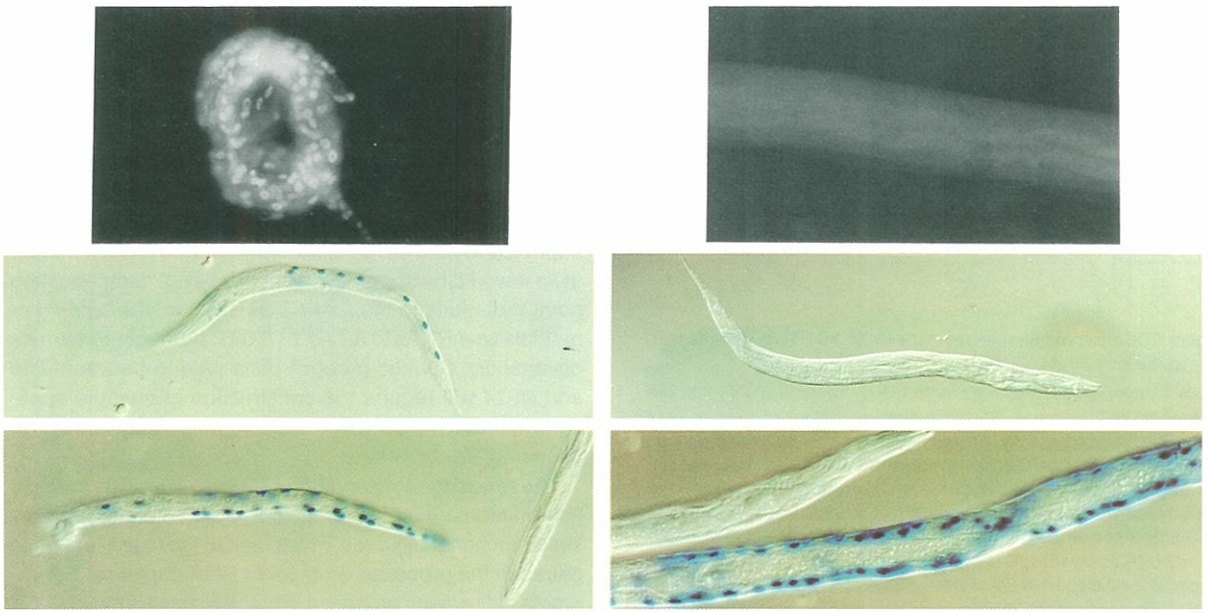

Figure 4. Regulation of *lin-14* in C. briggsae

(Top) Immunofluorescent staining of Lin-14p in C. briggsae. Animals were fixed and stained with anti-Lin-14p antibody raised to C. elegans Lin-14p (Ruvkun and Giusto, 1989), then detected with goat anti-rabbit fluorescein labeled secondary antibody. (Left) An L1 stage C. briggsae animal shows Lin-14p in most cells. (Right) An L2 stage C. briggsae animal displays no detectable *lin-14* staining, as observed in C. elegans.

(Middle) Temporal down-regulation of β-galactosidase activity from the C. elegans *col-10–lacZ–lin-14* 3′UTR reporter gene in C. briggsae. (Left) L1 stage. (Right) L4 stage.

(Bottom) No significant temporal regulation of β-galactosidase activity from the C. elegans *col-10–lacZ–unc-54* 3′UTR reporter gene in C. briggsae. (Left) L1 stage. (Right) L4 stage.

that shows partial gradient generating activity (Table 1; Figure 5). However, additional conserved elements besides those complementary to *lin-4* are present in this 802 nt region. The 124 nt *lin-14* 3′UTR fragment assayed in the pC10L14/124 construct also shows partial temporal gradient generating activity. This 124 bp fragment bears three *lin-4* complementary elements, and these elements account for all of the conserved sequences in this region. These data suggest that the *lin-4* complementary sites mediate part, but not all, of the temporal gradient-generating activity of the *lin-14* 3′UTR.

Discussion

The *lin-14* 3′UTR Is Necessary and Sufficient for Posttranscriptional Temporal Regulation by *lin-4*

We have shown that during wild-type development, the level of Lin-14p drops by a factor of at least 10 between the L1 and later larval stages, while *lin-14* RNA levels remain relatively constant (see Figure 1). Thus, posttranscriptional regulation, rather than changes in *lin-14* transcription or mRNA stability, causes the down-regulation of Lin-14p during and after the L1 stage.

The location of both *lin-14(gf)* mutations in the 3′UTR argues that sequences in the 3′UTR are necessary for temporal regulation of *lin-14* (Wightman et al., 1991). At post-L1 stages, Lin-14p levels are 4-fold higher in the *lin-14(n536gf)* and 7-fold higher in the *lin-14(n355gf)* mutants than they are in wild type (Figure 1A). In contrast, transcript levels do not change significantly in the same staged samples (Figure 1B). Therefore, we conclude that the negative regulatory sequences in the 3′UTR that are disrupted by these mutations control a process other than *lin-14* transcription or transcript stability.

The *lin-14* 3′UTR is sufficient to confer posttranscriptional temporal regulation on an unrelated reporter transcript. Reporter gene expression is temporally down-regulated about 20-fold more with the *lin-14* 3′UTR than with the control *unc-54* 3′UTR (Table 1; Figure 2). As in the case of the normal *lin-14* down-regulation, the *lin-14* 3′UTR reporter gene is down-regulated posttranscriptionally (Figure 3).

Like *lin-14(gf)* mutations, loss-of-function *lin-4* mutations result in inappropriately high levels of Lin-14p at late larval stages (Figure 1A). Because a *lin-4* null mutation does not appreciably affect *lin-14* RNA levels (Figure 1B), the temporal regulation of Lin-14p abundance by *lin-4* must also occur at a posttranscriptional step. Furthermore, a reporter gene that bears the *lin-14* 3′UTR is not temporally regulated in the absence of *lin-4*, showing that *lin-4* regulates *lin-14* via the *lin-14* 3′UTR (Table 1; Figure 2). These data support the model that *lin-4* negatively regulates *lin-14* via elements located in the *lin-14* 3′UTR to inhibit expression posttranscriptionally at post-L1 larval stages.

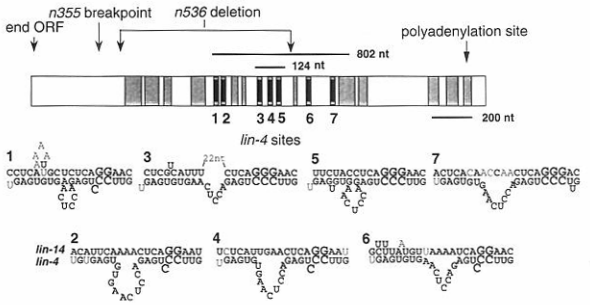

Figure 5. Conserved Sequences in the *lin-14* 3′UTR Are Complementary to the *lin-4* RNAs

(Top) A representation of regions in the C. elegans 3′UTR that are conserved in C. briggsae. Shown in gray are regions of 10 nt or more that are conserved exactly. Shown in black overlaid on gray are conserved regions that are complementary to the *lin-4* RNAs. These potential *lin-4*-binding sites are numbered to correspond to those shown in detail below. The deletion breakpoints and polyadenylation site for the C. elegans sequence are labeled above the line. The region of the *lin-14* 3′UTR assayed in pC10L14/802 and pC10L14/124 is also shown. (Bottom) Predicted *lin-4–lin-14* RNA duplexes in the 3′UTR of a *lin-14* mRNA. The stacked G::C base pairs in the core element and the potential *lin-4* bulged C at RNA duplexes 1, 2, 4, and 6 are shown in large type. *lin-4* and *lin-14* nucleotide positions that are conserved between C. elegans and C. briggsae are indicated in bold type. Only the 5′-most nucleotides of the *lin-4* sequence are shown.

Seven Conserved Elements in the *lin-14* 3′UTR Are Complementary to the *lin-4* Regulatory RNAs

lin-4 encodes two overlapping untranslated RNA molecules (Lee et al., 1993). We have identified seven copies of a 14–19 base sequence motif in the *lin-14* 3′UTR that is complementary to a portion of the *lin-4* transcripts (Figure 5). The locations of the *lin-14(gf)* and *lin-4* loss-of-function mutations, the detailed pattern of sequence conservation relative to these complementary regions, and our functional analysis of these regions in temporal gradient formation all favor the model that the *lin-4* and *lin-14* RNAs form an RNA duplex that negatively regulates post-transcriptional processing, transport, or translation of the *lin-14* mRNA. First, all the *lin-4* complementary elements are deleted from the *lin-14* transcript in the *lin-14(n355gf)* mutant, which is a strong gain-of-function allele. Second, 5 of the 7 *lin-4* complementary elements in the *lin-14* 3′UTR are deleted by the *lin-14(n536gf)* mutation, and this is a relatively weak allele. Third, a reporter gene bearing three of the *lin-4* complementary sites shows partial temporal gradient generating activity. Fourth, all seven of the proposed *lin-4* complementary elements in the *lin-14* 3′UTR are completely conserved between C. elegans and C. briggsae in the 8–10 nt core sequence, as are all but one of the *lin-4* nucleotide positions proposed to base pair to the *lin-14* 3′UTR (Lee et al., 1993). The flanking complementary regions also show significant, though not complete, conservation: five changes in a total of 50 base pairing positions. Fifth, the *lin-4(ma161)* mutation causes a C to U transition in the region of *lin-4* RNA that is predicted to be base paired (Lee et al., 1993). Thermodynamic calculations, assuming the RNA duplexes shown in Figure 5, suggest that the substitution of a G::U base pair for the G::C base pair in a *lin-4(ma161)–lin-14(+)* RNA duplex would decrease the free energy of each of the three GGG/CCC RNA duplexes (sites 3, 5, and 7) by 2.6 kcal/mol, lowering the binding constant of each by a factor of 100 (Turner et al., 1988).

Because we found no evolutionary variation of the *lin-4* and *lin-14* RNA sequences in the base paired regions, we could not use evolutionary covariation data to support the RNA duplex model. However, because the *lin-4* RNA is expected to bind seven sites in the *lin-14* 3′UTR, a mutant in *lin-4* would be suppressed only by seven compensating point mutations in the *lin-14* 3′UTR. Thus, the binding of multiple *lin-4* RNAs to the *lin-14* 3′UTR probably constrains covariation. Genetic proof of base pairing between *lin-4* and *lin-14* will require the construction of multiple mutations in the *lin-14* gene that are complementary to a corresponding *lin-4* mutation.

The sequence conservation of both *lin-4* and the multiple complementary regions in the *lin-14* 3′UTR highlights possible functional residues, in addition to those that are base paired in the proposed *lin-4–lin-14* RNA duplexes. For example, all seven proposed RNA duplexes loop out the conserved residues ACCUC from the *lin-4* RNA (Lee et al., 1993), while a corresponding loop of *lin-14* RNA varies from 0 to 22 nt (see Figure 5). In addition, for both C. briggsae and C. elegans, while three of the proposed *lin-4/lin-14* RNA duplexes would base pair perfectly in the core region, four of these sites would base pair with the *lin-4* RNAs only by bulging out one of the conserved *lin-4* C residues in the core sequence (sites 1, 2, 4, and 6 in Figure 5). The *lin-4(ma161)* mutation is expected to substitute a U for the bulged C in these duplexes, which could disrupt the function of those *lin-4–lin-14* RNA duplexes. Because all of these features of the proposed RNA duplexes are conserved between C. elegans and C. briggsae, we favor the proposition that they are essential for *lin-4*-mediated regulation of *lin-14*. For example, the conserved loops or bulges on the duplex could be recognized by accessory proteins or may be essential to any catalytic activity the *lin-4–lin-14* RNA duplex may possess. An analogous conserved and reiterated bulged C RNA duplex in the vertebrate transferrin receptor mRNA 3′UTR has been shown to mediate binding to an iron–sulfur protein that regulates transferrin mRNA stability (Klausner et al., 1993).

If all seven sites in the *lin-14* mRNA must be occupied by *lin-4* to achieve posttranscriptional down-regulation of *lin-14*, the *lin-4* level should be much more abundant than the *lin-14* mRNA level at post-L1 stages. Indeed, we found that a high copy *lin-14* 3′UTR reporter transgene with 50 times the gene dosage and β-galactosidase activity at each stage was temporally down-regulated about 100-fold in wild type when compared with a low copy transgene (Table 1). Thus, the *lin-4* RNA either must be present in great excess or be catalytic.

To establish how the *lin-4–lin-14* RNA duplex actually inhibits Lin-14p production, it is essential to discern where these RNAs first encounter each other. Clearly, if it takes place in the nucleus, polyadenylation and nuclear export are possible regulatory mechanisms, whereas interaction in the cytoplasm would favor direct translational control.

There are examples of posttranscriptional regulation

mediated by double-stranded RNA. Mammalian viral double-stranded RNA structures have been found to activate a kinase that deactivates host, but not viral, protein synthesis (Edery et al., 1989). Such a mechanism would be required to act in cis in the case of *lin-14*. In Xenopus and in Bombyx, antisense RNAs that are transcribed from the same DNA template in the opposite orientation from the target mRNA base pair and direct covalent modification of target sense mRNAs (Kimelman and Kirschner, 1989; Skeiky and Iatrou, 1991). Alternatively, the binding of *lin-4* RNA molecules may upset regulation of poly(A) tail length or ribosome binding (Sachs and Davis, 1989; Wickens 1990). Whatever mechanism is used, it does not depend on 5′ sequences peculiar to the *lin-14* mRNA, because the *lin-14* 3′UTR can also down-regulate translation of a hybrid *col-10–lacZ–lin-14* mRNA.

Multiple Elements in the *lin-14* 3′UTR Generate a Temporal Gradient of Lin-14p

The correlation between the level of Lin-14p and the stage-specific fates in various heterochronic mutants suggests that the level of Lin-14p forms a temporal gradient: relatively high levels of Lin-14p, for example, at the L1 stage in wild type or at all stages in the *lin-14(n355gf)* mutant, specifies an L1 fate, whereas intermediate level of Lin-14p, for example during the late L1 stage of wild type or at post-L2 stages in the weaker *lin-14(n536gf)* mutant, specifies L2 fate. Consistent with the weaker gain-of-function phenotype for *lin-14(n536)*, we observe less elevation of Lin-14p levels at late stages in this mutant than in the *lin-14(n355)* mutant (4-fold elevated levels versus 7-fold elevated levels; see Figure 1). Two potential *lin-4*-binding sites remain in the *lin-14(n536)* 3′UTR and may mediate the residual down-regulation.

In addition to the *lin-4*-complementary sites, other sequences are required for generation of the Lin-14p temporal gradient. Reporter genes bearing all seven of the *lin-4* complementary sites, but not other conserved regions in the *lin-14* 3′UTR, show partial gradient generating activity (see Table 1; Figure 5). In addition, a slight Lin-14p temporal gradient remains in the *lin-4(e912)* null mutant (see Figure 1A), suggesting that additional factors and sites not dependent on *lin-4* can partially mediate *lin-14* temporal gradient formation. Thus, the *lin-14* 3′UTR is analogous to other complex 3′UTRs that posttranscriptionally generate developmental gradients in Drosophila pattern formation genes (Irish et al., 1989). Multiple conserved elements in the 3′UTRs of these mRNAs appear to mediate spatial regulation (MacDonald, 1990; Wharton and Struhl, 1991).

Generation of a Temporal Gradient of Lin-14p by the Antisense *lin-4* RNA

A model for the regulation of Lin-14p in wild-type animals emerges from these data. At late embryonic and early L1 stages, the *lin-14* mRNA is actively produced and is translated to protein at high levels, directing the execution of L1-specific cell lineages. We have shown that the down-regulation of Lin-14p is triggered by feeding during the L1 stage (Arasu et al., 1991). We suggest that after this feeding trigger, the *lin-4* RNA reaches a concentration sufficient to bind to multiple sites in the 3′UTR of the *lin-14* transcript and inhibits a posttranscriptional step, resulting in the decline in Lin-14p levels.

We favor the model in which the seven sites in the *lin-14* 3′UTR bind to the *lin-4* RNAs in a cooperative manner to control the down-regulation of Lin-14p levels during the L1 and later stages. Synergistic binding by multiple *lin-4* molecules could generate a sharp down-regulation in the Lin-14p level at a particular *lin-4* RNA concentration during the L1 stage, for example, if binding one *lin-4* RNA changes the *lin-14* mRNA secondary structure to expose another *lin-4*-binding site and so on. In this way, a monotonic increase in *lin-4* RNA level during the L1 stage could generate a steeper gradient or steps in Lin-14p levels to regulate the temporal sequence of cell fates. Thus, the full complement of *lin-4*-binding sites may contribute to the shape of the temporal gradient in Lin-14p.

Experimental Procedures

Staging of Animals

Prior to starvation, mixed-staged animals were rinsed from plates with water and passed three times through a 20 mm filter that allows only L1 and early L2 animals to pass. Part of this early stage preperation was frozen immediately at −70°C. The remainder was allowed to develop to the L2 and later stages and was frozen. The population distribution of these preparations was as follows:

	L1	L2	L3	L4	Ad
Wild type early	89%	11%	0%	0%	0%
Wild type late	6%	72%	19%	3%	0%
lin-4(e912) early	71%	29%	0%	0%	0%
lin-4(e912) late	1%	78%	16%	5%	0%
lin-14(n355) early	89%	11%	0%	0%	0%
lin-14(n355) late	10%	38%	40%	12%	0%
lin-14(n536) early	88%	12%	0%	0%	0%
lin-14(n536) late	3%	46%	40%	11%	0%

Staged preparations from transformed strains bearing *lacZ* fusion constructs were prepared from eggs allowed to hatch overnight in phosphate-buffered saline. A portion of the hatched L1 animals was frozen, and the remainder was fed until the L4 stage.

Western Blot and RNAase Protection Analysis

Laemmli loading buffer was added directly to frozen staged animals, and a standard Western blotting procedures were used. Western blots were probed with a monoclonal antibody to *myo-1* (Miller et al., 1986) and a polyclonal antibody to *lin-14* (Ruvkun and Giusto, 1989). For detection of *lin-14* transcripts, cDNA clone 518 (Wightman et al., 1991) was transcribed in vitro to yield a 233 nt antisense probe. The *myo-1* probe is specific to this myosin isoform (Dibb et al., 1989) and was transcribed in vitro to yield a 58 nt antisense probe. Quantitation of both Western blots and RNAase protections was performed by scanning appropriate exposures on Kodak XAR film with a Kratos SD 3000 spectrodensitometer and a Hewlett-Packard 3390A integrator. For each experiment, the sum of the *lin-14* bands in each sample was divided by the myosin bands to obtain a value for *lin-14* normalized to myosin.

Construction of *lacZ* Expression Plasmids

pC10U54 (from V. Ambros) is a translational fusion of a 1.2 kb *col-10* promoter fragment fused to the ATG of *lacZ* in the pPD21.28 expression vector that utilizes an *unc-54* 3′UTR (Fire et al. 1990). A 1.8 kb fragment (position 19847–21637; Wightman et al., 1991) that includes the last 24 codons of the *lin-14* coding sequence, the entire 1.6 kb *lin-14* 3′UTR, and 130 bp of genomic DNA 3′ to the putative *lin-14* polyadenylation site, replaced the *unc-54* 3′UTR in pC10U54 to generate pC10L14. pC10L14 was found to contain a single A to G mutation at position 20808, which substitutes a G:U base pair for an A:U base

pair at the 3′ most position of the *lin-4–lin-14* RNA duplex number 5. Clone pC10L14-1 was constructed by replacing a BsmI-XhoI fragment bearing the mutation with the same fragment from wild type. pC10L14/124 was constructed from the *lin-14* 3′UTR region corresponding to *lin-4* complementary sites 3, 4, and 5, synthesized with flanking restriction sites, and cloned into the *unc-54* 3′UTR upstream of the polyadenylation site. Plasmid pC10L14/802 was constructed similarly, except that PCR primers with flanking restriction sites were used to amplify wild-type DNA as shown in Figure 5. All reporter gene 3′UTRs were sequenced.

Transgenic Reporter Genes

Constructs were coinjected with the marker plasmid pRF4, which bears a mutant *rol-6* collagen gene and allows identification of transgenic animals. Gonads of adult hermaphrodites of genotype *rol-6(n1270e187)*, which increases the penetrance of the dominant Rol phenotype, were microinjected with 200 μg/ml pRF4 and 2 μg/ml of *col-10–lacZ*–3′UTR fusion construct (Mello et al., 1991). The high copy transgene arrays were isolated by injecting pRF4 at 100 μg/ml and pC10L14 at 100 μg/ml. Extrachromosomal arrays were integrated by nonhomologous recombination with 3800 R or 4100 R from a cobalt or cesium source. Integrants were backcrossed to wild-type animals twice to remove any unlinked mutations.

β-Galactosidase Assays

β-Galactosidase activity was assayed using a chlorophenol red–β-D-galactopyranoside substrate (Simon and Lis, 1987). Activity was calculated by dividing the change in A_{574} over time by the amount of total protein in each extract. For strains bearing nonintegrated transgene arrays, where only a fraction of the animals carry the transgene array, this proportion was used to normalize β-galactosidase activity. Extracts made from Escherichia coli strain JM 83, on which worms were fed or wild-type C. elegans were fed, this strain yielded no detectable activity in this assay. X-Gal staining of whole-mount C. elegans were done as described (Krause et al., 1990).

Cloning and Sequencing of the C. briggsae *lin-14* Clone

A C. briggsae genomic library (from D. Baillie) was screened with ^{32}P-labeled 3.8 EcoRI fragment (positions 17866–21621; Wightman et al., 1991; Figure 1) and washed at low stringency (55°C, 2× SSC). Sequences were aligned with the GCG BestFit program.

Acknowledgments

The *lin-4* complementary sites in the *lin-14* 3′UTR were identified through the collaboration of our lab with the Ambros Lab. We also thank R. Feinbaum, V. Ambros, and members of the lab for discussion and comments on the manuscript. We thank D. Miller, B. Meyer, A. Sluder, and K. O'Donnell for reagents and protocols; D. Bartel and J. Szostak for advice on RNA secondary structure; B. Reinhart for help in finishing the sequence; and J. Gatto for technical assistance. The Caenorhabditis Genetic Center provides many strains and resources. We acknowledge the support of National Institutes of Health (GM44619) and Hoechst Aktiengesellschaft. G. R. is partially supported by an American Cancer Society faculty research award.

Received August 6, 1993; revised September 24, 1993.

References

Ambros, V. (1989). A hierarchy of regulatory genes controls a larva-to-adult developmental switch in C. elegans. Cell *57*, 49–57.

Ambros, V., and Horvitz, H. R. (1984). Heterochronic mutants of the nematode *Caenorhabditis elegans*. Science *226*, 409–416.

Ambros, V., and Horvitz, H. R. (1987). The *lin-14* locus of *Caenorhabditis elegans* controls the time of expression of specific postembryonic developmental events. Genes Dev. *1*, 398–414.

Arasu, P., Wightman, B., and Ruvkun, G. (1991). Temporal regulation of *lin-14* by the antagonistic action of two other heterochronic genes, *lin-4* and *lin-28*. Genes Dev. *5*, 1825–1833.

Chalfie, M., Horvitz, H. R., and Sulston, J. E. (1981). Mutations that lead to reiterations in the cell lineages of C. elegans. Cell *24*, 59–69.

Dibb, N. J., Brown, D. M., Karn, J., Moerman, D. G., Bolten, S. L., and Waterston, R. H. (1985). Sequence analysis of mutations that affect the synthesis, assembly and enzymatic activity of the *unc-54* myosin heavy chain of *Caenorhabditis elegans*. J. Mol. Biol. *183*, 542–551.

Dibb, N. J., Maruyama, N., Krause, M., and Karn, J. (1989). Sequence analysis of the *C. elegans* myosin heavy chain family. J. Mol. Biol. *205*, 603–613.

Edery, I., Petryshyn, R., and Sonenberg, N. (1989). Activation of double-stranded RNA-dependent kinase (dsl) by the TAR region of HIV-1 mRNA: a novel translational control mechanism. Cell *56*, 303–312.

Fire, A., Harrison, S. W., and Dixon, D. (1990). A modular set of lacZ fusion vectors for studying gene expression in *Caenorhabditis elegans*. Gene *93*, 189–198.

Irish, V., Lehmann, R., and Akam, M. (1989). The *Drosphila* posterior group gene nanos functions by repressing hunchback activity. Nature *338*, 646–648.

Kimelman, D., and Kirschner, M. W. (1989). An antisense mRNA directs the covalent modification of the transcript encoding fibroblast growth factor in Xenopus oocytes. Cell *59*, 687–696.

Klausner, R. D., Rouault, T. A., and Harford, J. B. (1993). Regulating the fate of mRNA: the control of cellular iron metabolism. Cell *72*, 19–28.

Krause, M., Fire, A., Harrison, S. W., Priess, J., and Weintraub, H. (1990). CeMyoD accumulation defines the body wall muscle cell fate during C. elegans embryogenesis. Cell *63*, 907–919.

Lee, R. C., Feinbaum, R. L., and Ambros, V. (1993). The C. elegans heterochronic gene *lin-4* encodes small RNAs with antisense complementarity to *lin-14*. Cell, this issue.

MacDonald, P. M. (1990). Bicoid mRNA localization signal: phylogenetic conservation of function and RNA secondary structure. Development *110*, 161–171.

Mello, C., Kramer, J. M., Stinchcomb, D., and Ambros, V. (1991). Efficient gene transfer in *C. elegans*: extrachromosomal maintenance and integration of transforming sequences. EMBO J. *10*, 3959–3970.

Miller, D. M., Stockdale, F. E., and Karn, J. (1986). Immunological identification of the genes encoding the four myosin heavy chain isoforms of *Caenorhabditis elegans*. Proc. Natl. Acad. Sci *83*, 2305–2309.

Nüsslein-Volhard, C. (1991). Determination of the embryonic axes of *Drosophila*. Development (Suppl.) *1*, 1–10.

Ruvkun, G., and Giusto, J. (1989). The *Caenorhabditis elegans* heterochronic gene *lin-14* encodes a nuclear protein that forms a temporal developmental switch. Nature *338*, 313–319.

Sachs, A. B., and Davis, R. W. (1989). The poly(A) binding protein is required for poly(A) shortening and 60S ribosomal subunit-dependent translation initiation. Cell *58*, 857–867.

Simon, J. A., and Lis, J. T. (1987). A germline transformation analysis reveals flexibility in the organization of heat shock consensus elements. Nucl. Acids Res. *15*, 2971–2988.

Skeiky, Y. A., and Iatrou, K. (1991). Developmental regulation of covalent modification of double stranded RNA during silkmoth oogenesis. J. Mol. Biol. *218*, 517–527.

Turner, D. H., Sugimoto, N., and Freier, S. M. (1988). RNA structure prediction. Ann. Rev. Biophys. Biophys. Chem. *17*, 167–192.

Wharton, R., and Struhl, G. (1991). RNA regulatory elements mediate control of Drosophila body pattern by the posterior morphogen nanos. Cell *67*, 955–967.

Wickens, M. (1990). In the beginning is the end: regulation of poly(A) addition and removal during early development. Trends Biochem. Sci. *15*, 320–324.

Wightman B., Bürglin, T. R., Gatto, J., Arasu, P., and Ruvkun, G. (1991). Negative regulatory sequences in the *lin-14* 3′- untranslated region are necessary to generate a temporal switch during *Caenorhabditis elegans* development. Genes. Dev. *5*, 1813–1824.

Zucker-Aprison, E., and Blumenthal, T. (1989). Potential regulatory elements of nematode vitellogenin genes revealed by interspecies sequence comparison. J. Mol. Evol. *28*, 487–496.